International Journal of Advancements in Mechanical and Aeronautical Engineering – IJAMAE 2018

Volume 5 : Issue 1- [ISSN : 2372-4153] - Publication Date: 25 June, 2018

Temperature Control of a Regasification System for LNG-fuelled Marine Engines

[Gun-Baek So and Gang-Gyoo Jin]

***Abstract*—This paper presents a nonlinear PID (NPID) controller which controls the glycol temperature of a regasification system for LNG-fuelled engines. The NPID controller has a parallel structure of linear PD action and nonlinear I action. A nonlinear function is employed to scale the error as input of the integral and implemented as a Takagi-Sugeno (T-S) fuzzy model. The controller parameters are optimally tuned by assuming that it is operated in both warming-up and running modes, and the parameters are switched according to the operation mode. Furthermore, the stability problem of the overall system is verified based on the circle criterion. A set of simulation works is carried out to validate the efficiency of the proposed controller.**

***Keywords*—NPID controller, regasification system, T-S fuzzy model, circle criterion**

I. Introduction

Excessive use of fossil fuels resources is adding several types of greenhouse gases which make the Earth warmer. Emissions from ship's exhausts contribute to global climate change, too. The International Maritime Organization (IMO) has adopted regulations to reduce the emission of air pollutants from international shipping, such as carbon dioxide (CO_2), nitrogen oxides (NOx), and sulphur oxides (SOx) under Annex VI of the 1997 MARPOL protocol [1,2].

Meanwhile, large engine manufacturers, such as MAN B&W and Wartsila, have been developing LNG-fuelled engines [3,4]. The use of LNG requires special equipment which can handle cryogenic temperatures (–162°C) and designing technologies of high-pressure dual fuel (HPDF) engines. HPDF engines work on diesel cycle in gas mode. To use cryogenic liquefied natural gas (LNG) as fuel, it has to be converted to gas at around 30~45°C, and this process is called LNG regasification.

Recently some studies have been done to control the temperature of shell-tube type heat exchangers. Vinaya et al. [5] proposed a discrete model predictive control algorithm, and Pandey et al. [6] proposed a PI-type fuzzy controller. Sivakumar et al. [7] investigated a method of combining neurofuzzy control with the PID control technique, and Sarabeevi et al. [8] addressed the problem associated with using a PID controller based on an internal model.

Gun-Baek So/PhD candidate
Dept. of Convergence Study on the OST, KMOU
Korea

Gang-Gyoo Jin/Professor
Dept. of IT, Korea Maritime and Ocean University (KMOU)
Korea

However, many industrial processes are highly nonlinear and their parameters change during operation. Although a fixed-gain controller is effective in a limited operating range, its performance degrades and may become unstable in some cases when it is out of this range. This problem can be solved, to some extent, by introducing nonlinear elements in the PID control structure. Some forms of nonlinear PID controllers have been studied for industrial processes. They can be categorized into two types. One is the nonlinear PID controller introduced by Korkmaz et al. [9] and Isayed [10], whose gains are gradually changed based on error and/or error rate. The other is the nonlinear PID controller introduced by Seraji [11] and Zaidner et al. [12], where a nonlinear gain in cascade with a linear PID controller produces the scaled error. These methods presented rather satisfactory results in different control environments, but further improvements are needed.

This paper presents a nonlinear PID controller which controls the outlet temperature of glycol on the secondary loop of a regasification system for LNG-fuelled engines. The NPID controller combines the linear PD action with a filter term in derivative action and nonlinear I action. A nonlinear function, employed in the I action to scale the error, is described by a Takagi-Sugeno (T-S) fuzzy model. As the proposed controller operates in two modes, two sets of the parameters are tuned by a genetic algorithm (GA) from the viewpoint of minimizing the integral of absolute error (IAE) performance index. Since the introduction of a nonlinear function causes the stability problem of the feedback system, it is analyzed using the circle criterion. To validate the effectiveness of the proposed method, a set of simulation works are performed.

II. A Heat Exchanger System

A regasification system for LNG-fuelled marine engines is shown in Fig. 1.

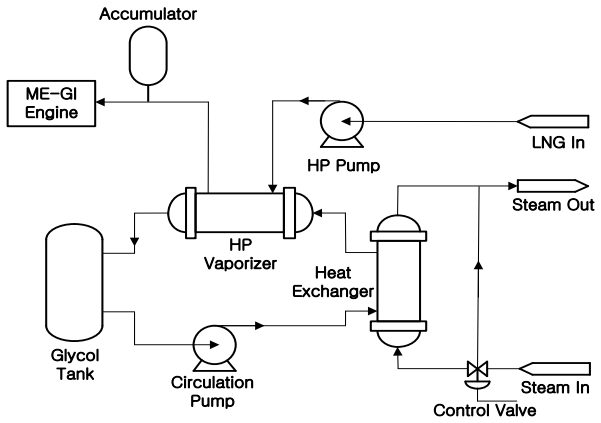

Figure 1. A regasification system for LNG-fuelled marine engines.

International Journal of Advancements in Mechanical and Aeronautical Engineering – IJAMAE 2018
Copyright © Institute of Research Engineers and Doctors , SEEK Digital Library
Volume 5 : Issue 1- [ISSN : 2372-4153] - Publication Date: 25 June, 2018

The regasification system is divided into the primary and secondary loops. After pumping cryogenic LNG on the primary loop to approximately 250-300 bar, it is heated in a high-pressure vaporizer to the gas state of 30~45°C and this gas is then fed to the engine cylinder through an injector. When LNG is vaporizing, it receives thermal energy from glycol as an intermediate heating medium. Meanwhile, on the secondary loop, the glycol cooled down in the vaporizer is reheated by hot steam supplied to the heat exchanger.

The objective of the proposed controller is to maintain the outlet temperature of glycol by controlling the amount of steam supplied to the heat exchanger on the secondary loop. The transfer function of each subsystem can be expressed as follows [8, 13]:

I/P converter and diaphragm valve

$$G_v(s) = \frac{K_{ip}K_v}{1+T_v s}, \tag{1}$$

heat exchanger

$$G_h(s) = \frac{K_h}{1+T_h s}, \tag{2}$$

disturbance

$$G_d(s) = \frac{K_d}{1+T_h s}, \tag{3}$$

measurement sensor

$$H(s) = \frac{K_s}{1+T_s s}, \tag{4}$$

where K_{ip}, K_v, and T_v the constant of the I/P converter (psi/mA), the gain (kg/sec·psi) and time constant (sec) of the diaphragm valve, respectively; K_h and T_h the gain (°C·sec/kg), the time constant (sec) of the heat exchanger; K_d the gain of the disturbance model; K_s and T_s the gain (mA/°C) and the time constant (sec) of the measurement sensor, respectively.

III. Controller Design

A. *Design of a Nonlinear PID Controller*

To control the glycol temperature of the heat exchanger, the proposed controller forms a combination of linear PD block and nonlinear I block. The overall block diagram that combines the controller and the plant is shown in Fig. 2.

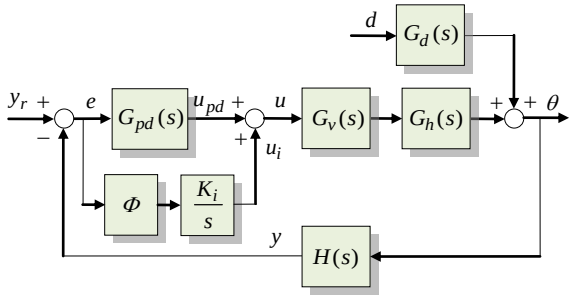

Figure 2. Overall control system.

In Fig. 2, y_r, θ, y, and d denote the reference input, output, measurement output, and disturbance, respectively; e the error which is defined as $e = y_r - y$; u_{pd} and u_i the outputs of the PD controller and I controller, respectively.

The PD controller with a first-order filter is expressed by

$$G_{pd}(s) = \frac{U_{pd}(s)}{E(s)} = K_p + \frac{K_d s}{1+T_f s}. \tag{5}$$

where K_p and K_d are the proportional and derivative gains, respectively; $T_f = K_d/(NK_p)$ the filter time constant; and the maximum derivative gain N is an empirically determined constant between 8 and 20, and $N = 10$ is used [14].

The integral provides necessary action to eliminate steady-state error caused by the P controller and disturbances. Once a large change in set-point occurs or a large disturbance applies, the integral of the error keeps increasing fast and overshoot occurs. When the error is so small, the integral action is still collecting error until it is large enough to eliminate steady-state error completely. Therefore, when the error is large, the integral of the error is preferred to take small values to prevent overshoot and when the error is small, the integral of the error is preferred to take large values to remove offset quickly.

For this, a nonlinear integral action is employed:

$$u_i(t) = K_i \int \Phi(e) \cdot e(t) dt, \tag{6}$$

where $\Phi(e)$ is a nonlinear function which provides a nonlinearly-scaled error according to e.

$\Phi(e)$ is described by a Takagi-Sugeno (T-S) fuzzy model as:

$$R_1: \text{if } e \text{ is } F_1, \text{ then } \Phi(e) = k_1, \tag{7a}$$

$$R_2: \text{if } e \text{ is } F_2, \text{ then } \Phi(e) = k_2, \tag{7b}$$

$$R_3: \text{if } e \text{ is } F_3, \text{ then } \Phi(e) = k_1, \tag{7c}$$

where e is the input variable of the fuzzy system, F_i(i=1,2,3) fuzzy sets defined on e, and k_1 and k_2 are user-defined positive constants ($0 \le k_1 < k_2$). Meanwhile, the membership functions of F_1, F_2, and F_3 are shown in (8)-(10):

$$F_1(e) = \begin{cases} 1, & e \le -3\sigma \\ -e/3\sigma, & -3\sigma < e \le 0 \\ 0, & elsewhere \end{cases}, \tag{8}$$

$$F_2(e) = \exp\left(-\frac{e^2}{2\sigma^2}\right), \tag{9}$$

$$F_3(e) = \begin{cases} e/3\sigma, & 0 \le e < 3\sigma \\ 1, & e \ge 3\sigma \\ 0, & elsewhere \end{cases}, \tag{10}$$

where σ is the standard deviation of $F_2(e)$ and a user-defined parameter.

Given the input e, the final output $\Phi(e)$ of the fuzzy system is inferred by

$$\Phi(e) = \sum_i^3 \alpha_i \Phi_i(e) / \sum_i^3 \alpha_i = \sum_i^3 \alpha_i k_i / \sum_i^3 \alpha_i, \tag{11}$$

where the weight α_i implies the membership grade of e in $F_i(e)$. When the fuzzy sets are defined, they are overlapped such that $\sum_i^3 \alpha_i > 0$ is always true for all e.

B. *Tuning of the NPID Controller*

In general, a regasification system for LNG-fuelled main engines is operated in two modes: warming-up and running modes. Since, in the warming-up mode, the set-point (SP) is gradually changed until the glycol temperature comes up to the operating temperature, the controller should be tuned to favor SP tracking. However, in the running mode, since the SP is fixed at the operating temperature, the controller should be tuned to favor disturbance rejection.

Therefore, two sets of the NPID controller parameters are tuned by a GA such that the following IAE criterion is minimized:

$$J(K_p, K_i, K_d, \alpha) = \int_0^{t_f} |e(t)|dt \ , \qquad (12)$$

where t_f is a sufficiently large time.

IV. Stability Analysis

In this study, for the stability analysis of a nonlinear system, circle stability theory is applied. The circle criterion can be performed for the nonlinear system in Fig. 2 that can be decomposed into a linear block $G(s)$ and a nonlinear block Φ as shown in Fig. 3. Here, y_r is considered as constant and d as zero for convenience.

Here, the linear transfer function $G(s)$ is then

$$G(s) = \frac{K_i G_v(s) G_h(s) H(s)}{s[1 + G_{pd}(s) G_v(s) G_h(s) H(s)]} = \frac{1}{s}\frac{V(s)}{W(s)} \ , \qquad (13)$$

where $V(s) = K_i G_v(s) G_h(s) H(s)$, $W(s) = 1 + G_{pd}(s) G_v(s) G_h(s) H(s)$ and $\deg(V(s)) < \deg(W(s))$.

Definition 1 A memoryless function $\Phi : \Re \rightarrow \Re$ is said to belong to the sector $[k_1, k_2]$, if there exist two non-negative numbers k_1 and $k_2 (k_2 > k_1)$ such that

$$k_1 e \le \Phi \le k_2 e, \forall e \in \Re \ . \qquad (14)$$

In (14), $\Phi(0) = 0$ and the relationship of $\Phi \cdot e \ge 0$ is always true. Geometrically, $\Phi \in [k_1, k_2]$ exists between the two straight lines $k_1 e$ and $k_2 e$, that is, it exists in the first and third quadrants, as depicted in Fig. 4.

Theorem 1 (Circle criterion) Consider the feedback system in Fig. 3 where $G(s)$ is stable (i.e., it has all its poles in the left half-plane with one pole at the origin). Assume that the nonlinearity Φ satisfies a sector condition $[k_1, k_2]$, $k_1 < k_2$. Then the system is absolutely stable if the following condition is satisfied:

$$\mathrm{Re}\left[\frac{1 + k_2 G(j\omega)}{1 + k_1 G(j\omega)}\right] > 0, \ \omega \in \Re \ . \qquad (15)$$

Proof: Theorem 1 can be proved by using loop transformation, a Lyapunov function and the Kalman-Yakubovich-Popov equations. See [15].

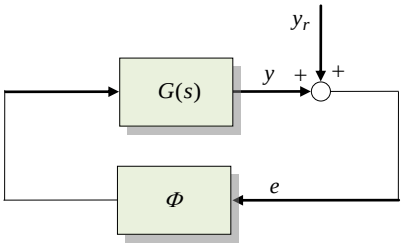

Figure 3. Equivalent control system.

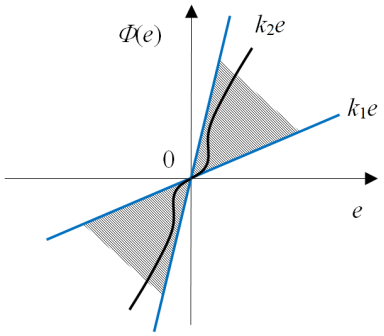

Figure 4. Geometrical representation of the sector $[k_1, k_2]$.

Lemma 1 Consider the system in Fig. 3 where $G(s)$ is stable and $\Phi \in [k_1, k_2]$. Then the system is absolutely stable if one of the following conditions is satisfied:

1) If $0 < k_1 < k_2$, then the Nyquist plot of $G(j\omega)$ does not penetrate the disk $D(k_1, k_2)$ having as diameter the segment $[-1/k_1, -1/k_2]$ located on the x-axis.

2) If $0 = k_1 < k_2$, then the Nyquist plot of $G(j\omega)$ is located on the right of a vertical line defined by $\mathrm{Re}(s) = -1/k_2$.

3) If $k_1 < 0 < k_2$, then the Nyquist plot of $G(j\omega)$ is within the disk $D(k_1, k_2)$.

Proof: Suppose that $G(j\omega) = u + jv$. In the case of $0 < k_1 < k_2$, (15) can be rewritten as:

$$\mathrm{Re}\left[\frac{1/k_2 + G(j\omega)}{1/k_1 + G(j\omega)}\right] = \frac{(1/k_2 + u)(1/k_1 + u) + v^2}{(1/k_1 + u)^2 + v^2} > 0 \ .$$

Rearranging the above inequality with the factor that the denominator is never zero yields

$$[u + \frac{1}{2}(\frac{1}{k_1} + \frac{1}{k_2})]^2 + v^2 > [\frac{1}{2}(\frac{1}{k_1} - \frac{1}{k_2})]^2 \ .$$

This inequality implies that the Nyquist plot of $G(j\omega)$ locates the outside of the circle with the center of $-0.5(1/k_1 + 1/k_2) + j0$ and a radius $0.5(1/k_1 - 1/k_2)$ and never enter the disk $D(k_1, k_2)$, shown in Fig. 5(a).

In the case of $0 = k_1 < k_2$, (15) can be rewritten as

$$\mathrm{Re}[1 + k_2 G(j\omega)] = 1 + k_2 u > 0 \ .$$

Rearranging the above inequality yields

$$\mathrm{Re} G(j\omega) = u > -1/k_2 \ .$$

This inequality implies that the Nyquist plot of $G(j\omega)$ lies to the right of a vertical line defined by $\mathrm{Re}(G(j\omega))= -1/k_2$, shown in Fig. 5(b).

In the case of $k_1 < 0 < k_2$, (15) can be easily rewritten as:

$$[u+\frac{1}{2}(\frac{1}{k_1}+\frac{1}{k_2})]^2+v^2<[\frac{1}{2}(\frac{1}{k_1}-\frac{1}{k_2})]^2$$

This inequality implies that the Nyquist plot of $G(j\omega)$ lies in the interior of the disk $D(k_1, k_2)$, shown in Fig. 5(c).

Theorem 2 Consider the mapping of the T-S fuzzy system in Fig. 3, $\Phi(e)$. If $k_1= 0$ and $k_2= 1$, then $\Phi(e)$ belongs to the sector [0, 1].

Proof: From the result of the fuzzy inference in (11), $\alpha_i \geq 0$(i= 1,2,3) and the fact that $\alpha_1+\alpha_2+\alpha_3 \neq 0$, clearly we have

$$\Phi(e) \geq \frac{\alpha_1 k_1+\alpha_2 k_1+\alpha_3 k_1}{\alpha_1+\alpha_2+\alpha_3} e = k_1 e ,$$

and also

$$\Phi(e) \leq \frac{\alpha_1 k_2+\alpha_2 k_2+\alpha_3 k_2}{\alpha_1+\alpha_2+\alpha_3} e = k_2 e .$$

Since we have $0 = k_1 e \leq \Phi(e) \leq k_2 e= 1$, hence $\Phi(e)$ belongs to the sector [0, 1].

To demonstrate that the feedback system in Fig. 3 is absolutely stable, applying the parameters in Table I with the choice of $k_1= 0$ and $k_2= 1$ to (13) gives $V(s)= 0.006s + 0.359$ and $W(s)= 14.973s^5 + 906.987s^4 + 420.715s^3 + 92.043s^2 + 9.134s$. It can be easily verified that the linear part $G(s)$ has five stable poles at 0, –0.2096, –60.1100, and –0.1281 ± j0.1789. We can apply the second case of the Lemma 1.

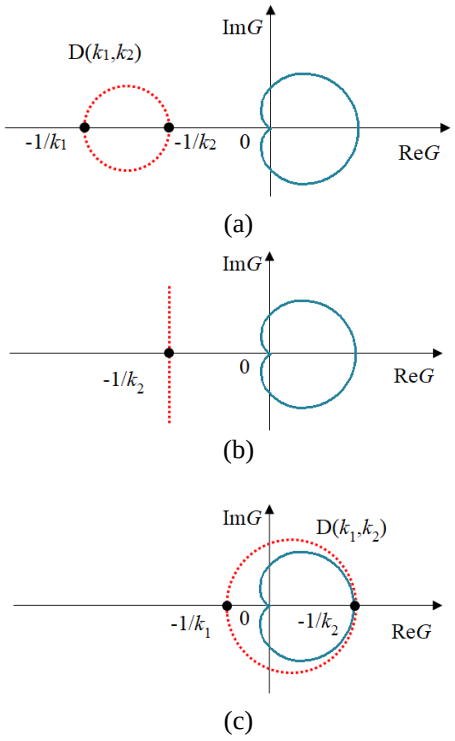

Figure 5. Disk $D(k_1,k_2)$ and Nyquist plot of $G(j\omega)$.

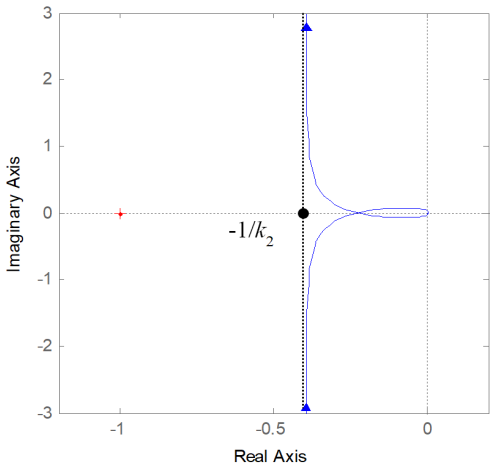

Figure 6. Nyquist plot of $G(j\omega)$.

Clearly, the choice of k_2 is not unique. The Nyquist plot of $G(j\omega)$ shown in Fig. 6 is on the right of the vertical line $\mathrm{Re}(s)= -0.395$. Therefore, $-1/k_2= -0.395$, that is, $k_2= 2.532$. This means that the system is absolutely stable for all values of k_2 less than 2.532. Hence, we can conclude that the feedback system is absolutely stable for all nonlinearities $\Phi \in [0, 1]$.

v. Simulation Results

A set of simulation works are performed to verify the effectiveness of the proposed method on the plant with the parameters in Table I. The results are then compared with those of the PID controller tuned by the Ziegler-Nichols (Z-N), Tyreus-Luyben (T-L), and Aström methods [14]. An optimal tuning of the proposed NPID controller is set by a GA.

TABLE I. PARAMETERS OF THE PLANT

Parameter	Value
K_{ip}	0.75 psi/mA
K_v	0.4/3 kg/sec·psi
T_v	3 sec
K_h	12.5 °C·sec/kg
T_h	30 sec
K_s	0.2 mA/°C
T_s	10 sec
K_d	1

TABLE II. TUNED CONTROLLER PARAMETERS

Method	Gains				Remarks
	K_p	K_i	K_d	α	
Proposed	32.535	1.435	195.565	0.106	Tracking
	55.364	0.679	263.918	0.577	Disturbance rejection
Z-N	44.882	3.122	161.296	-	K_u= 76.3 P_u= 28.8
T-L	34.682	0.548	158.270		
Aström	15.168	0.429	134.186		

The linear PID controller gains are tuned based on inducing ultimate vibration. The ultimate gain K_u and the ultimate period P_u are 76.3 and 28.8, respectively.

A. Response to Set-point Change

During warming-up, engineers preheat the coolant, lubricant, and fuel oil of an engine to the desired temperatures to prepare the engine for startup. In the case of LNG-fuelled engines, the engineers must increase the temperature gradually over time because the liquid LNG must be raised slowly to the normal temperature of 30~45 °C. At this time, the controller must ensure that the output follows the changed SP well. To check the SP tracking performance of the controller, a test of changing the SP to 40 °C while the system output temperature is maintained at 35 °C is conducted and the result is compared with those of the other methods.

Fig. 7 shows that the proposed method gives better results in terms of both swiftness and closeness of responses. The response of the Z-N method is the poorest, whereas the T-L and Aström methods show a long settling time. For quantitative comparison, the rise time $t_r = t_{95}$-t_5, peak time t_p, overshoot M_p, 2% settling time t_s, and the integral of absolute error (IAE) were calculated and listed in Table III. It can be clearly seen that the proposed method exhibits smaller overshoot and remarkably reduced settling time than the other methods.

B. Response to Disturbance Changes

Once the warming-up process finishes, the engineer no longer changes the SP and sets the controller to running mode. When the controller is switched, the parameters of the NPID controller are reset. After that, the role of the controller is to make the output temperature return to the SP as quickly as possible whenever there is a disturbance.

While the system is operating at 40 °C, a simulation of changing the temperature of glycol returning to the heat exchanger from 30 °C to 35 °C is performed. Fig. 8 shows the responses.

To quantitatively measure the performances of the four methods, the perturbation peak M_{peak}, the time t_{peak} at this peak, the recovery time t_{rcv} that the output temperature returns to the SP after a disturbance is applied, and the IAE are calculated. $M_{peak} = | y_{max} - y_r |$ or $| y_{min} - y_r |$, and t_{rcv} means the time required for the recovery of y to less than 2 % of y_r. Table IV outlines the calculated quantitative performances. The proposed method provides more improved performance as compared to the other methods. M_{peak} is samller by 2~3 times, and t_{rcy} is shorter by 2~3 times.

C. Response to Noise Rejection

A simulation was performed to verify the robustness of the proposed controller against noises. It was assumed that there were noises in the range of –1.2~1.2°C when the outlet temperature of glycol was measured through a sensor.

Fig. 9 shows that the proposed method has no changes in responses, but the responses of the other methods are severely distorted due to the ideal derivative action.

D. Response to Parameter Changes

Next, the robustness of the proposed controller against parameter changes of the plant was verified. It was assumed that the gain K_h and the time constant T_h of the heat exchanger changed most severely. A simulation of increasing and decreasing these values by around 10 % of the nominal value was performed (see Figs. 10-11).

It is shown in the figures that the proposed method is more robust to the parameter changes than the other methods.

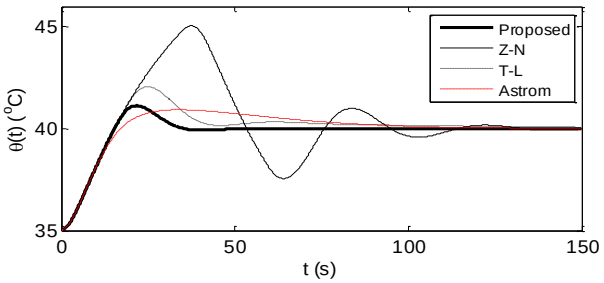

Figure 7. Responses of the four methods when the SP is step-wisely changed from 35 to 40 °C.

TABLE III. QUANTITATIVE COMPARISON OF THE SP TRACKING PERFORMANCE

Method	SP tracking performance				
	t_r	t_p	M_p	t_s	*IAE*
Proposed	12.606	21.800	22.570	33.615	55.220
Z-N	12.606	37.550	101.128	128.338	204.837
T-L	12.606	25.000	41.258	128.756	92.602
Aström	13.855	34.000	18.663	103.056	88.902

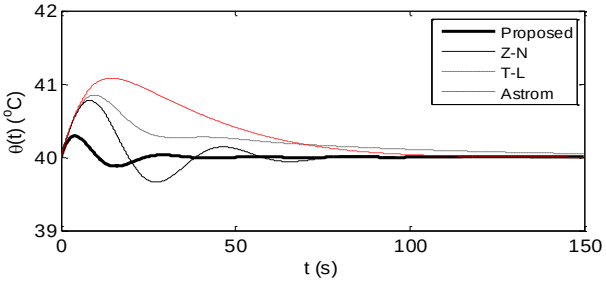

Figure 8. Responses when a step-type disturbance d is applied (d= 30→35 °C).

TABLE IV. DISTURBANCE REJECTION PERFORMANCES WHEN d=30→35°C IS CHANGED

Method	Disturbance rejection performance			
	t_{peak}	M_{peak}	t_{rcy}	*IAE*
Proposed	3.950	0.292	45.881	3.300
Z-N	8.250	0.776	90.691	16.354
T-L	9.650	0.848	150.000	33.538
Aström	14.500	1.080	107.730	46.704

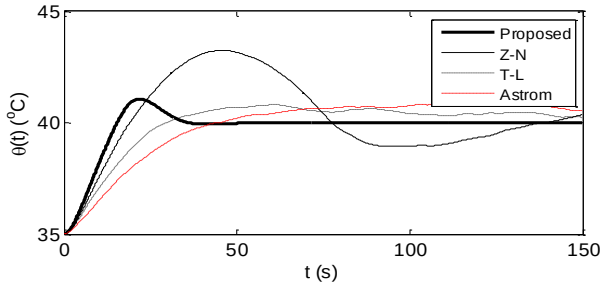

Figure 9. Responses of the four methods when the SP is step-wisely changed from 35 to 40 °C with Gaussian noise N(0,0.01^2).

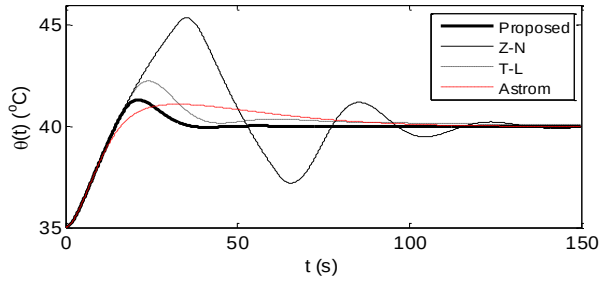

Figure 10. Response comparison to parameter changes (K_h = 12.5→13.75, T_h = 30→33) while y_r = 35→40 ºC.

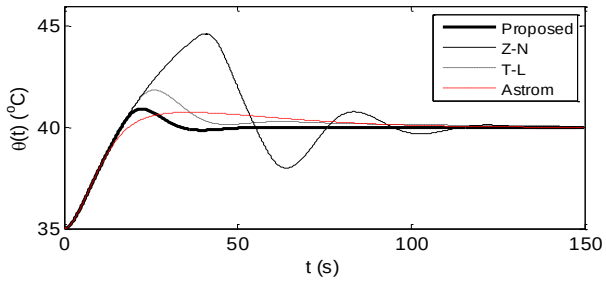

Figure 11. Response comparison to parameter changes (K_h= 12.5→11.25, T_h = 30→27) while y_r = 35→40 ºC.

VI. Conclusion

In this study, an NPID controller was proposed to control the outlet temperature of glycol by throttling a diaphragm valve installed in the LNG regasification system. A nonlinear function implemented by the T-S fuzzy model plays the role of continuously scaling the error of as an input of the integral action so that the proposed controller can maintain satisfactory control performance despite environmental changes.

Two sets of the controller parameters were tuned assuming that the controller was operated in the warming-up and running modes. To validate the proposed method, the set-point tracking performance, robustness to noise and parameter change, and disturbance rejection performance were measured. Furthermore, the circle criterion was utilized to analyze the absolute stability of the nonlinear feedback system. The simulation results showed that the proposed controller outperformed all the other methods.

References

[1] S. Kumar, H. Kwon et al., "LNG: An eco-friendly cryogenic fuel for sustainable development," Applied Energy, vol. 88, no. 12, pp. 4264-4273, 2011.

[2] IMO, Green House GAS Emissions from Ships, Phase 1 Report, 2008.

[3] MAN Diesel & Turbo, ME-GI Duel Fuel MAN B&W Engines: A Technical, Operational and Cost-effective Solution for Ships Fuelled by Gas, 2012.

[4] S. Jafarzadeh, N. Paltrinieri, I. B. Utne and H. Ellingsen, "LNG-fuelled fishing vessels: A systems engineering approach," Transportation Research Part D, vol. 50, pp. 202-222, 2017.

[5] V. Vinaya Krishna, K. Ramkumar and V. Alagesan, "Control of Heat Exchangers Using Model Predictive Controller," Proc. of the 2012 IEEE Int. Conf. on Advances In Engineering, Science And Management, Tamil Nadu, India, pp. 242-246, 2012.

[6] M. Pandey, K. Ramkumar and V. Alagesan, "Design of Fuzzy Logic Controller for a Cross Flow Shell and Tube Heat-Exchanger," Proc. of the 2012 IEEE Int. Conf. on Advances In Engineering, Science And Management, Tamil Nadu, India, pp. 150-154, 2012.

[7] P. Sivakumar, D. Prabhakaran, and T. Kannadasan, "Temperature Control of Shell and Tube Heat Exchanger by Using Intelligent Controllers-Case Study," Int. J. of Computational Engineering Research, vol. 2, no. 8, pp. 285-291, 2012.

[8] G. M. Sarabeevi and M. L. Beebi, "Temperature control of shell and tube heat exchanger system using internal model controllers," 2016 Int. Conf. on Next Generation Intelligent Systems (ICNGIS), Kottayam, India, 2016.

[9] M. Korkmaz, O. Aydogdu, and H. Dogan, "Design and performance comparison of variable parameter nonlinear PID controller and genetic algorithm based PID controller," Proc. of 2012 IEEE Int. Symp. on Innovations in Intelligent Systems and Applications, Trabzon, Turkey pp. 1-5, 2012.

[10] B. M. Isayed and M. A. Hawwa, "A nonlinear PID control scheme for hard disk drive servo systems," Proc. of 2007 Mediterranean Conf. on Control & Automation, Athens, Greece, pp. 1-6, 2007.

[11] H. Seraji, "A New Class of Nonlinear PID Controllers," Proc. of IFAC Robot Control, Nantes, France, pp. 65-71, 1997.

[12] G. Zaidner, S. Korotkin, et al., "Non linear PID and its application in process control," Proc. of 2010 IEEE 26th Convention of Electrical and Electronics Engineers, Eliat, Israel, pp. 574-577, 2010.

[13] H. Afrianto, M. R.Tanshen et al., "A numerical investigation on LNG flow and heat transfer characteristic in heat exchanger," Int. J. of Heat and Mass Transfer, vol. 68, pp. 110-118, 2014.

[14] A. O'Dwyer, Handbook of PI and PID Controller Tuning Rules, Second Ed. Imperial College Press, London, UK, 2006.

[15] H. K. Khalil, Nonlinear Systems, Third Ed. Prentice Hall, New Jersey, USA, 2002.

About Author (s):

Gun-Baek So received his B.S. degree in Marine Engineering and M.S. degree in Control and Instrumentation Engineering from the Korea Maritime and Ocean University in 2009 and 2012, respectively. Currently he is a Ph.D. candidate in the Dept. of Convergence Study on the OST, KMOU. His research interests include process control.

Gang-Gyoo Jin received his B.S. degree in Marine Engineering from Korea Maritime University, an M.S. degree in Electrical, Electronic and Computer Engineering from the FIT, and a Ph.D. degree in Electrical, Electronic and Systems Engineering from the Cardiff University, in 1977, 1985 and 1996, respectively. His research interests include control and genetic algorithms.